Impact Assessment of Agro-Meteorological Drought Using Geo-Spatial Techniques. A Case Study of Southeastern Sindh-Pakistan

Saira Batool[1], Syed Amer Mahmood[2], Jahanzeb Qureshi[2], Amer Masood[2], Maryam Muhammad Ali[2], Zainab Tahir[2]
[1]Centre for Integrated Mountain Research
[2]Department of Space Science, University of Punjab Lahore
*Correspondence: sairabnaqvi5@gmail.com

Citation | Batool. S, Mahmood. S. A, Qureshi. J, Masood. A, Ali. M. M, Tahir. Z, "Impact Assessment of Agro-Meteorological Drought Using Geo-Spatial Techniques. A Case Study of Southeastern Sindh-Pakistan", IJIST, Special Issue pp 455-471, June 2024
Received | June 11, 2024 **Revised |** June 16, 2024 **Accepted |** June 20, 2024 **Published |** June 28, 2024.

The frequency of droughts is increasing as global temperatures rise. To effectively monitor drought conditions, it is crucial to use the appropriate index. In this study, the Standardized Precipitation Index (SPI) and Reconnaissance Drought Index (RDI) were applied to evaluate droughts. The tool "DrinC" was used to calculate the RDI for 3-, 6-, and 12-month periods (Oct-Dec, Oct-March, and Oct-Sept) from 1981 to 2020. RDI values between -1.0 and -2.5 indicated moderate to extreme droughts across all districts. The RDI for 3, 6, and 12 months highlighted significant drought years, including 1984, 1992, 1994, 2010, 2011, 2015, and 2019, showing reduced productivity during these periods. Dry conditions were prevalent at most stations between 1981 and 2020. In South-Eastern Sindh, Pakistan, this study also assessed changes in Land Surface Temperature (LST), Normalized Difference Vegetation Index (NDVI), and Soil Moisture Index (SMI) over the last four decades (1981-2020). Satellite data analysis showed that NDVI peaked in 1988 (+0.53) and hit its lowest in 2021 (+0.48). Similarly, SMI ranged from +1.1 in 1988 to +0.98 in 2021, while LST increased from 35.1°C in 1988 to 53.4°C in 2021. A negative correlation between SPI and RDI was observed through linear regression, confirming the effectiveness of both indices in assessing drought severity. These findings can inform the development of drought preparedness plans, helping to mitigate the impact of drought on various economic sectors.

Keywords: Climate change, RDI, SPI, Remote Sensing, NDVI, LST, SMI, Geospatial Techniques.

Introduction:

Drought is described as a prolonged period of below-average natural water availability occurring on a regional scale, and it can happen anywhere in the world [1][2]. Due to global warming caused by increased greenhouse gases, the frequency of droughts is expected to rise. Global warming is predicted to cause spatial and temporal fluctuations in water demand and availability [3]. Drought is a severe natural disaster that impacts multiple economic sectors and severely affects the lives of the poor worldwide. Most scientists agree that drought has multiple causes. Its definition varies: agriculturists associate it with insufficient moisture (often called "effective precipitation") [4], which negatively impacts crop yields, meteorologists define it as prolonged low rainfall, and hydrologists as reduced water runoff. Climate change, the main driver of drought, highlights the roles of evapotranspiration (ET), rainfall, and water runoff [5]. Droughts, often complex and global in nature, frequently affect large populations and vast areas [6].

Climate change projections suggest that rising global temperatures will influence evapotranspiration and specific air moisture levels, affecting atmospheric water storage and directly impacting the intensity, duration, and distribution of rainfall [7]. Meteorological drought, which affects weather and climate processes, can lead to hydrological drought by reducing surface and groundwater levels, lowering water supply, and degrading water quality. The cyclical drought pattern in Africa over many years has caused various severe consequences, such as mortality, crop failures, and food shortages [8]. According to one researcher [9], these conditions have led to malnutrition in several regions, causing hunger, disease, and population displacement. Between 1900 and 2010, drought was directly responsible for over ten million deaths. In Europe, the droughts of 2003 and 2006 reduced agricultural output, hindered navigation, and caused fatalities. The Mediterranean region's last major drought, lasting until 2008, had long-term effects by depleting groundwater resources and storage conditions.

Even with the possibility of increased precipitation and rising temperatures, droughts may still pose a significant challenge [10]. These could severely affect Pakistan's agro-climatic regions, particularly in arid areas. Sindh and Baluchistan are likely to face two to three water crises annually and are more vulnerable to drought than Punjab, Khyber Pakhtunkhwa, and Baluchistan. Various indicators are commonly used to assess drought, including the crop moisture index, vegetation condition index (VCI), temperature condition index (TCI), deciles index, and the standard water-level index (SWI) [11]. These indices estimate drought using large datasets, each offering a slightly different perspective. The standard precipitation index (SPI) is one of the most widely applied tools in regional drought studies [12]. The World Meteorological Organization (WMO) recommends using both the reconnaissance drought index (RDI) and the SPI to characterize drought conditions [13]. These tools allow drought visualization across different timescales. The RDI was chosen for this study because it accounts for water scarcity by incorporating both temperature and precipitation data [14]. The RDI is particularly useful for research on smaller spatial scales, while the SPI is more beneficial for studies across various timeframes.

Often, drought goes unnoticed for several years before its impact suddenly becomes evident [15]. People only recognize it once the damage has already begun. In Sindh, the frequency of droughts has increased due to changing weather patterns and rising pollution levels. To assist disaster mitigation managers and other stakeholders, this study examines historical drought variations in Sindh's districts, helping place current droughts in context.

Material and Methods:

Study Area:

The Sindh province of Pakistan is located in the southeast of the country, encompassing 23 districts. It lies between latitudes 25.8943° N and longitudes 68.5247° E, covering about 18% of Pakistan's total land area (140,914 km²). Sindh is bordered by the provinces of Baluchistan to

the north and Punjab to the northeast, and it shares its eastern boundary with the Indian states of Rajasthan and Gujarat. The province experiences extreme temperatures, with winter highs averaging 27.08°C and summer peaks reaching 43.32°C, alongside an average annual rainfall of 128.80 mm.

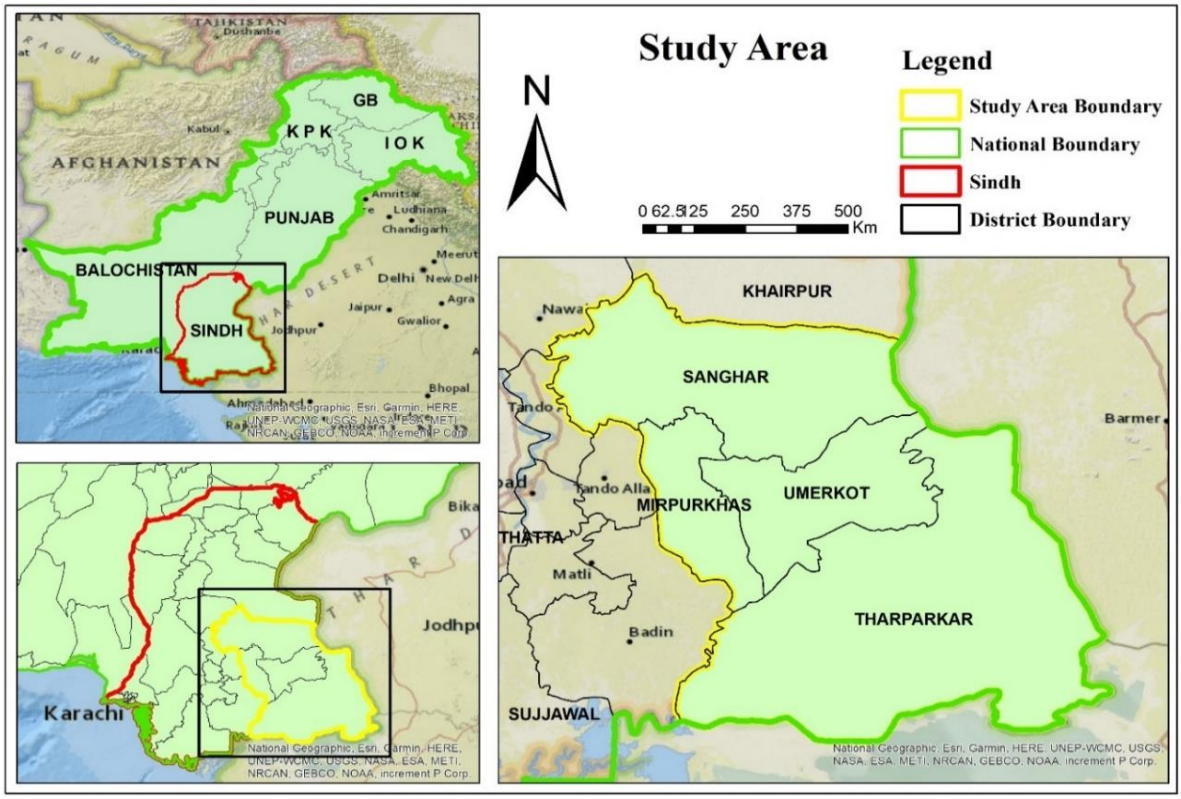

Figure 1: Map of Study Area

Data Acquisition:

Our research utilized temperature and average precipitation data from the meteorological department, covering the years 1981 to 2020. We calculated the Standard Precipitation Index (SPI) and Reconnaissance Drought Index (RDI). The DrinC (Drought Indices Calculator) tool was used to easily compute these indices for one year, six months, nine months, and three months, using gamma and log-normal methods, respectively. A relationship was observed between the RDI and SPI. However, according to a researcher [16], the RDI is derived by fitting the gamma distribution to annual rainfall and PET data. Geographic Information System (GIS) methods are critical for agricultural modelling, particularly for analyzing variables such as temperature, soil, and rainfall over space and time [17]. GIS interpolation techniques were employed to study the spatial distribution and frequency of droughts in the study area [18]. In this investigation, we used the IDW (Inverse Distance Weighting) interpolation method. Researchers also used vegetation and land surface temperature data to calculate the Soil Moisture Index. Landsat 8 satellite images, with a spatial resolution of 30m, were sourced from the USGS Earth Explorer website for this study. The red and near-infrared (NIR) bands were used to estimate the Normalized Difference Vegetation Index (NDVI), while the thermal infrared (TIR) bands were necessary for computing land surface temperature (LST) [19].

Standardized Precipitation Index (SPI):

The Standard Precipitation Index (SPI) was developed by fitting a probabilistic model to geographic rainfall data to monitor drought conditions [20]. This drought indicator helps distinguish between dry and wet seasons over various time periods in different parts of the world. SPI enables the calculation of drought frequency for any specific location over time [17].

The World Meteorological Organization (WMO) recommends using the SPI to measure rainfall amounts over a defined period. By transforming rainfall data into a normally distributed function, the average SPI for a given region and period is set to zero [21].

X stands for precipitation during a certain time period, and stands for probability density. f (x)=1/ ((_0)) x (-1) e(-x/) x>0 1 where and are the parameters defining the form and scale of respectively. SPI readings that are positive or negative represent greater or lesser rainfall than the norm. High negative SPI readings point to a very dry condition.

Reconnaissance Drought Index (RDI):

In 2005, Tsakiris and Vangelis developed the Reconnaissance Drought Index (RDI) for drought monitoring and assessment [17]. The RDI is based on the combination of total precipitation (P), which is observed, and potential evapotranspiration (PET), which is estimated. Due to its effectiveness, Hargreaves' method for estimating PET has been widely applied in semi-arid and arid regions [22]. The RDI can be calculated in three forms: the initial value RDI (k), the normalized RDI (nor), and the standardized RDI (std). These values are used in an equation, assuming a log-normal distribution, to assess and manage drought conditions.

RDIst (i) = y (i) - y / y 2

According to a researcher [23], \ (y(i) \) represents the natural logarithm of \ (ak (i) \), where \ (y \) is the arithmetic mean and \ (\sigma(y) \) is the standard deviation. Positive RDI values indicate wetter-than-average conditions, while negative RDI values signal drier conditions compared to the regional norm. Drought intensity is classified as moderate with an RDI of -1.0 and severe with an RDI of -2.0.

Table 1: Classification of droughts according to SPI and RDI values [17]

RDI and SPI	Classes
≥ 2.00	Extremely wet
1.5 to 1.99	Severely wet
1.0 to 1.49	Moderately wet
0.0 to 0.99	Normal
0.0 to −0.99	Mild drought
−1.00 to −1.49	Moderate drought
−1.50 to −1.99	Severe drought
≤ −2.00	Extreme drought

Calculation of LST NDVI and Soil Moisture Index (SMI):

The formula for calculating the Soil Moisture Index (SMI) [24] provides an accurate representation of the relationship between Land Surface Temperature (LST) and the Normalized Difference Vegetation Index (NDVI).

: $\boldsymbol{SMI} = (LSTmax - LST) / (LSTmax - LST\text{min})$ 3

The maximum and minimum surface temperatures for a given NDVI are referred to as LST max and LST min, respectively, where LST represents Land Surface Temperature. These values can be derived from satellite images, allowing us to determine the surface temperature of individual pixels at specific NDVI values. By solving the relevant equations, we can calculate both the maximum and minimum LSTs for the specified conditions.

$$\boldsymbol{LSTmax} = a1 * NDVI + b1 \quad 4$$

$$\boldsymbol{LSTmin} = a2 * NDVI + b2 \quad 5$$

The cold and warm sides of the dataset are defined by the current slopes and intercepts, where \(a\) and \(b\) are the actual variables obtained from regression analysis. Equation (1) is used to convert the digital number (DN) into radiance (LW/m²/sr), which is the first step in calculating the Soil Moisture Index (SMI).

$$\mathbf{L} = LSTmin + (((LSTmax - LSTmin) / (QCALmax - QCALmin)) * (\text{DN} - QCALmin)) \quad 6$$

The maximum and minimum quantization values, QCAL max and QCAL min, along with the Digital Numbers, are used to calibrate the number of pixels. Parameters LST min and

LST max are employed to measure spectral radiance. To determine the maximum and minimum values of Land Surface Temperature (LST), both NDVI and LST inputs must be evaluated. Using the thermal channels from Landsat 5 and Landsat 8, the equation calculates LST in Kelvin (K).

$$\mathbf{LST} = Tb \,/\, [1 + (\lambda * Tb/C2) * \ln(\varepsilon)] \quad 7$$

In the equation, \ (T_b \) represents the satellite's brightness temperature, \ (\lambda \) is the wavelength of the emitted radiation, \ (C_2 = 1.4388 \times 10^2 \text{ m K} \) is a constant, and \(\epsilon \) denotes emissivity. The Normalized Difference Vegetation Index (NDVI), derived from satellite data, is a metric used to evaluate plant health. By utilizing a high-resolution radiometer, scientists can assess whether vegetation is thriving or deteriorating. This method helps track changes in temperature, land use, and plant types. It can also be applied in risk analyses to identify plant groups that are vulnerable to drought and areas with inadequate water supply.

NDVI (Landsat 8 OLI): NIR=B5, R-B4 8

NDVI (Landsat 5 TM): NIR=B4, R=B3 9

Table 2: NDVI values for different types of cover

NDVI Range	Type of Cover
NDVI ≤ 0	Bare soil or water
0 to 0.2	Sparsely Vegetation
0.2 to 0.4	Less vegetation
0.4 to 0.6	Moderate Vegetation
0.6 to 0.8	Dense vegetation
0.8 to 1	Thick greenery

Linear Regression Analysis:

Linear regression is a statistical method used to analyze the relationship between two variables. It is the most frequently employed technique for investigating such relationships. Linear regression analysis, through its parametric approaches like the LR (slope) [25], reveals the typical rate of change over time for the variables of interest. If the average periodic change curve of the factors is positive, the trend in the dataset increases, and if negative, it decreases [26]. The RDI and SPI are useful for assessing meteorological droughts spanning three, six, nine, or twelve months. In the Sindh region, a significant correlation was found between RDI and SPI.

Results and Discussion:

Spatio Temporal Analysis of RDI:

The three distinct RDI periods (3, 6, and 12 months) were combined using inverse distance weighting (IDW) interpolation to create a geographical description of drought [27]. IDW data is reliable and avoids autocorrelation, as it is gathered for specific areas and time periods [28]. Geographic displays of RDI values were generated using ArcGIS 10.8, illustrating the length of the drought (Figures 9–11). The geospatial analysis focused on periods with RDI values. The interpolated images were produced based on the available data at the time.

Analysis of Three Months RDI Values:

The analysis reveals significant variation in RDI values across geographical areas affected by drought. Data indicate that Sindh experienced extreme drought only in 1993 and 2010, not across the entire study region. Severe droughts were widespread in 1984, 1988, 1992, 2010, and 2011. Numerous moderate droughts occurred in 1984, 1988, 1989, 1991, 1992, 1993, 2009, 2010, 2011, 2012, 2015, and 2019. Other years ranged from somewhat dry to exceptionally wet conditions. The Sindh region saw above-average rainfall in 2013 and 2020.

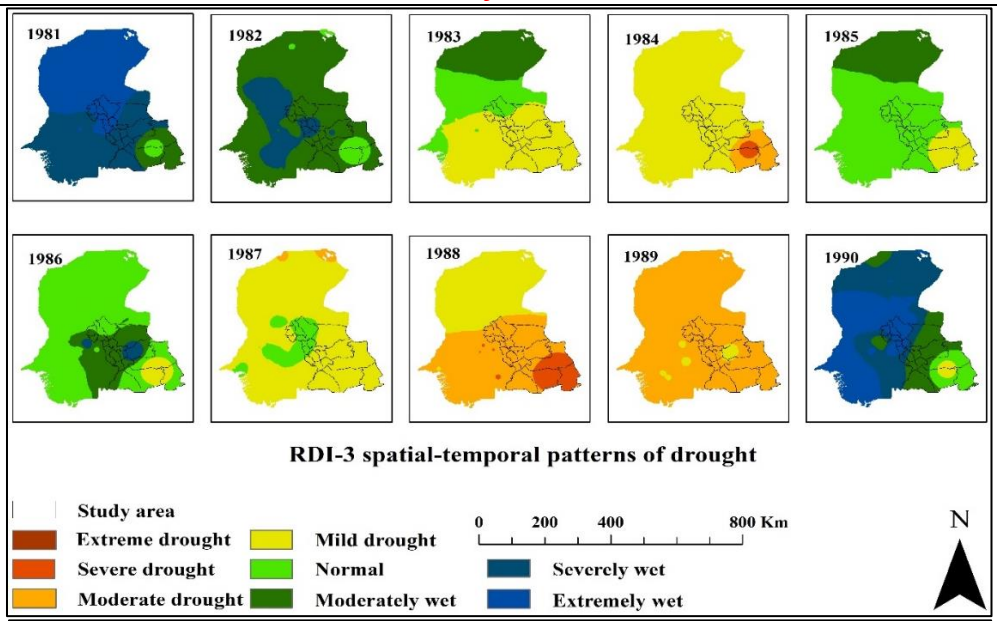
1981
1982
1983
1984
1985
1986
1987
1988
1989
1990
RDI-3 spatial-temporal patterns of drought
Study area
Extreme drought
Severe drought
Moderate drought
Mild drought
Normal
Moderately wet
Severely wet
Extremely wet
0 200 400 800 Km
N

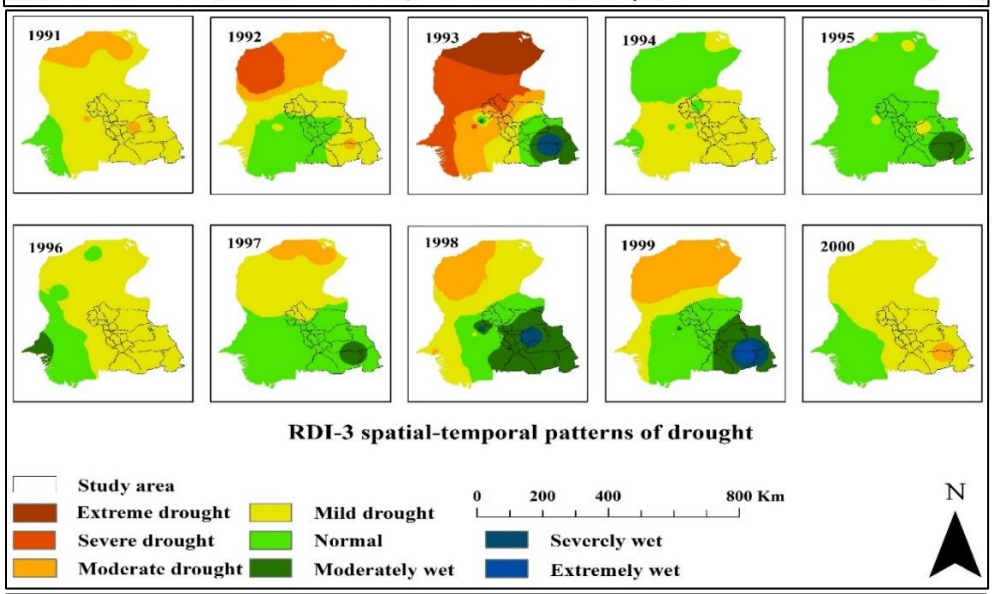
1991
1992
1993
1994
1995
1996
1997
1998
1999
2000
RDI-3 spatial-temporal patterns of drought
Study area
Extreme drought
Severe drought
Moderate drought
Mild drought
Normal
Moderately wet
Severely wet
Extremely wet
0 200 400 800 Km
N

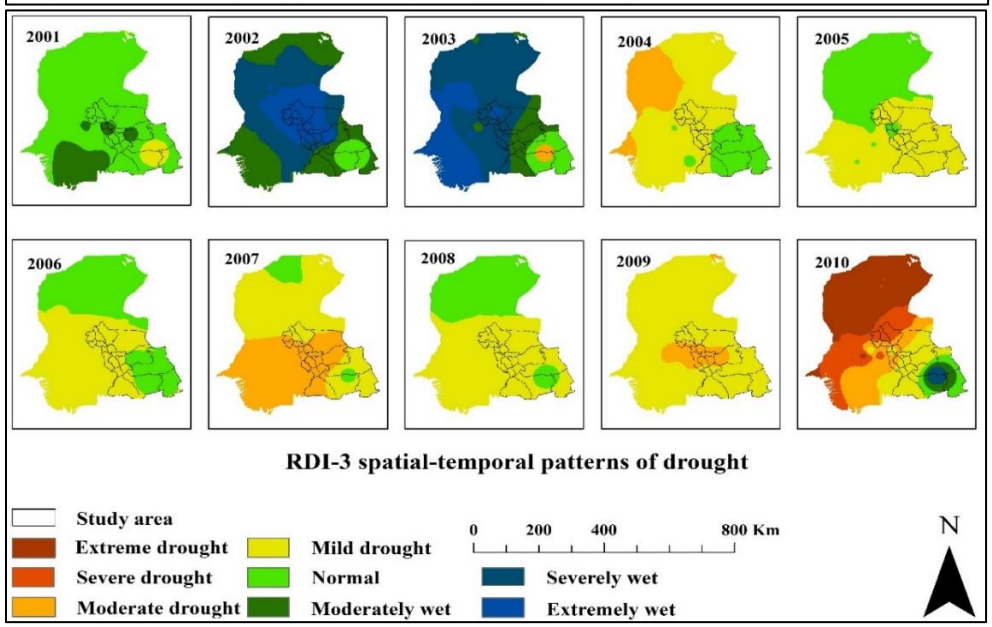
2001
2002
2003
2004
2005
2006
2007
2008
2009
2010
RDI-3 spatial-temporal patterns of drought
Study area
Extreme drought
Severe drought
Moderate drought
Mild drought
Normal
Moderately wet
Severely wet
Extremely wet
0 200 400 800 Km
N

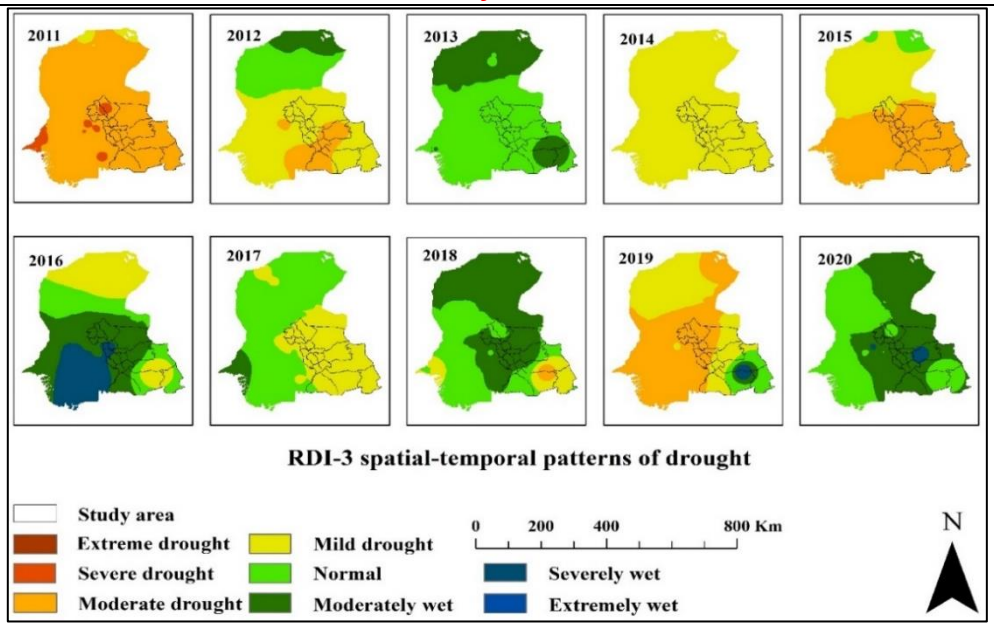

Figure 2: RDI-3 spatial-temporal patterns of drought for the years (1981–2020) based on RDI values

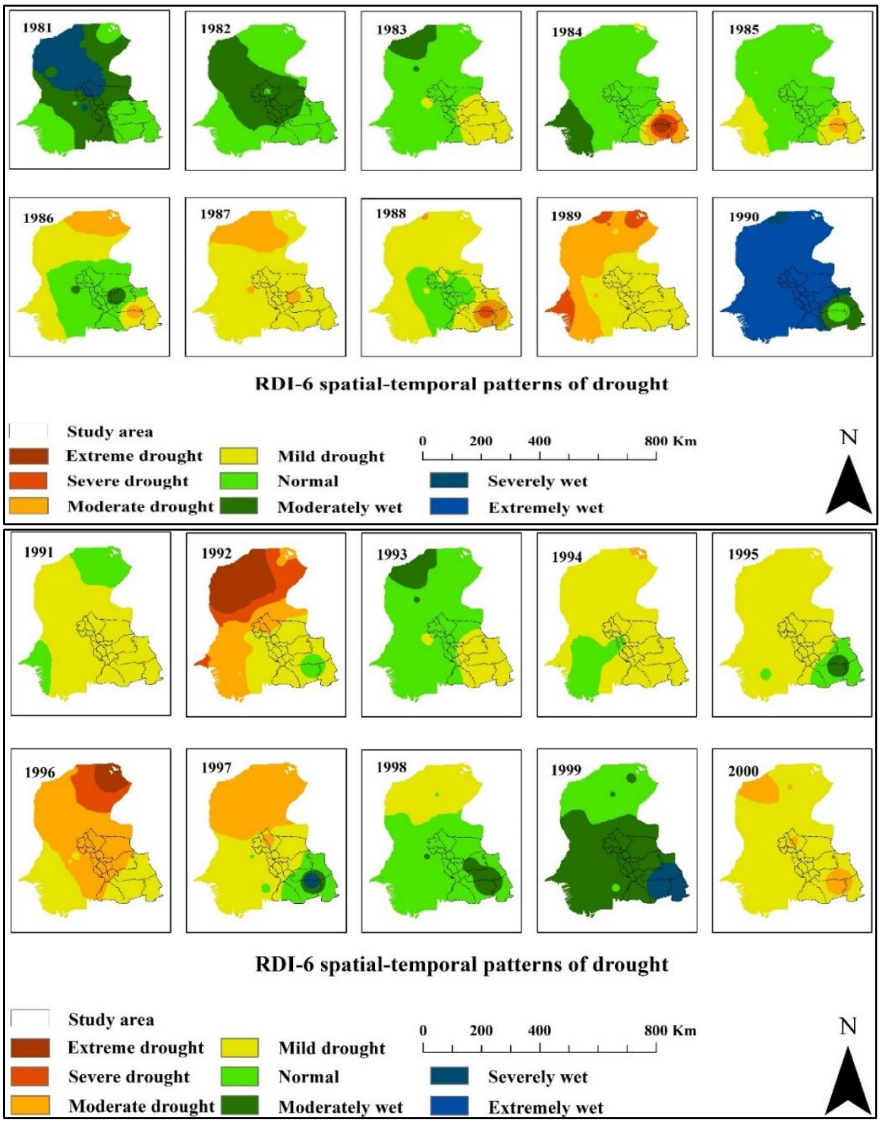

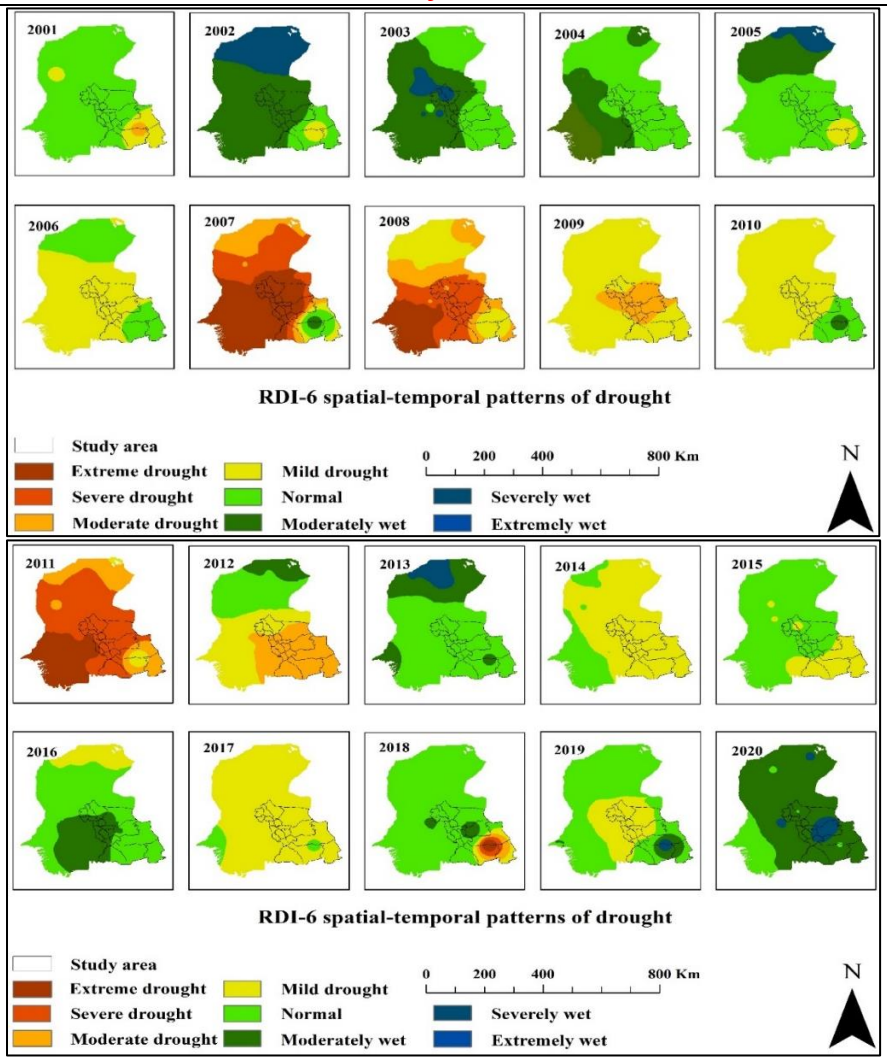

Figure 3: RDI-6 spatial-temporal patterns of drought for the years (1981–2020) based on RDI values

Analysis of Six Months RDI Values:

Based on the regional analysis of RDI-6 results, the study area experienced widespread drought effects ranging from mild to severe in approximately 22 out of 40 years. Extreme drought conditions were reported in the years 2007, 1984, and 2011. Over the past 16 years, most cities have experienced above-average rainfall, with the Sindh region being notably rainy each year. Extremely rainy weather was observed across the entire study region in 1990.

Analysis of 12 Months' RDI Values:

The spatial analysis of RDI-12 data indicates that the study area faced a range of mild-to-extremely wet drought conditions for about 27 years. Above-average rainfall was recorded in 1982, 1993, 1999, 2012, and 2015. Extreme and severe drought conditions were noted in 1987, 1991, 1992, 1997, 2002, 2010, and 2014. Moderate droughts occurred in 1986, 1991, 1997, and 2014. Notably, all districts experienced above-average rainfall in 1982 and 2015.

Correlation Between SPI and RDI:

The scatter plot of SPI values versus RDI is illustrated in Figures 5-8. The plot reveals that differences between the two indices tend to increase with longer time lags. Despite this, there is a notable consistency between the indices across all time scales. Our analysis indicates that the two indicators used for drought identification perform exceptionally well.

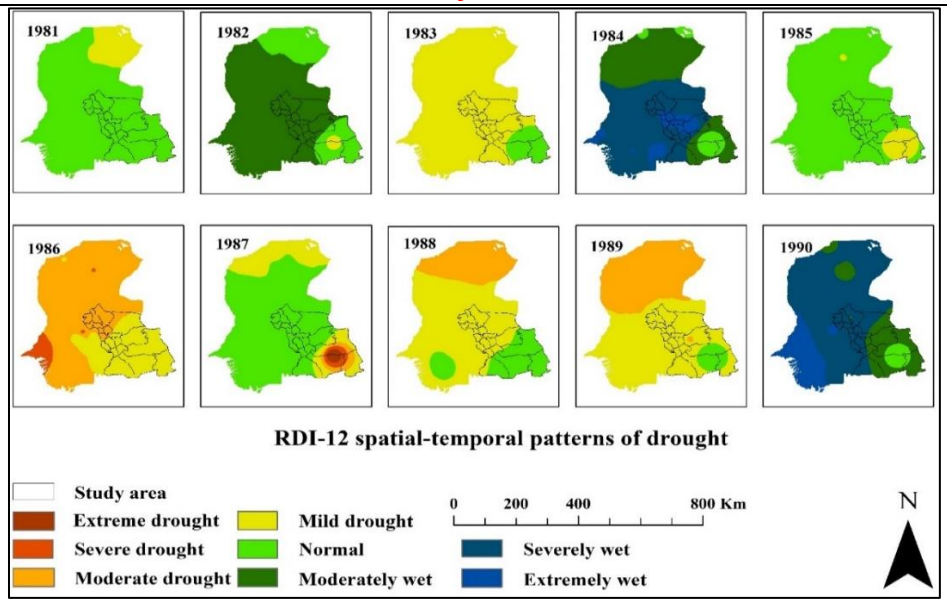
1981
1982
1983
1984
1985
1986
1987
1988
1989
1990
RDI-12 spatial-temporal patterns of drought
Study area
Extreme drought
Severe drought
Moderate drought
Mild drought
Normal
Moderately wet
Severely wet
Extremely wet
0 200 400 800 Km
N

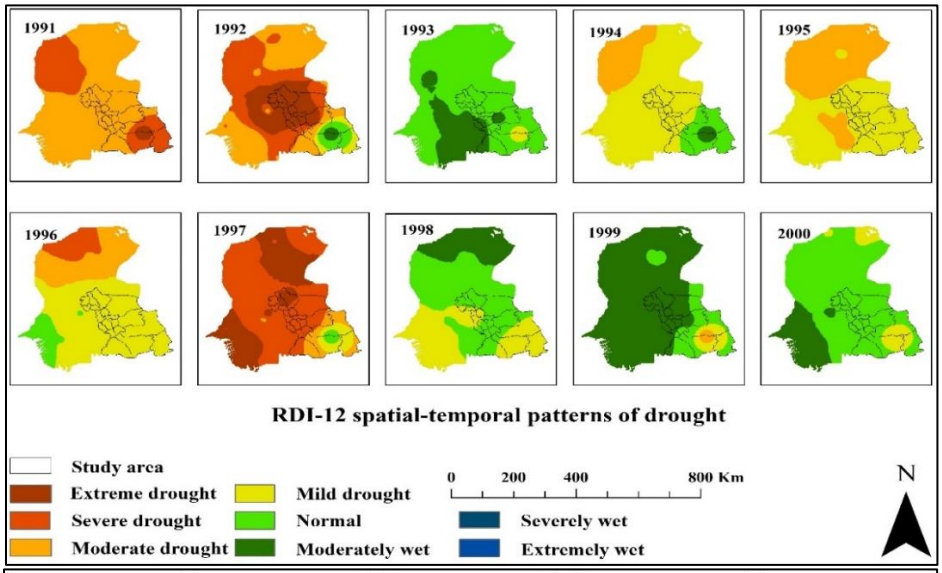
1991
1992
1993
1994
1995
1996
1997
1998
1999
2000
RDI-12 spatial-temporal patterns of drought
Study area
Extreme drought
Severe drought
Moderate drought
Mild drought
Normal
Moderately wet
Severely wet
Extremely wet
0 200 400 800 Km
N

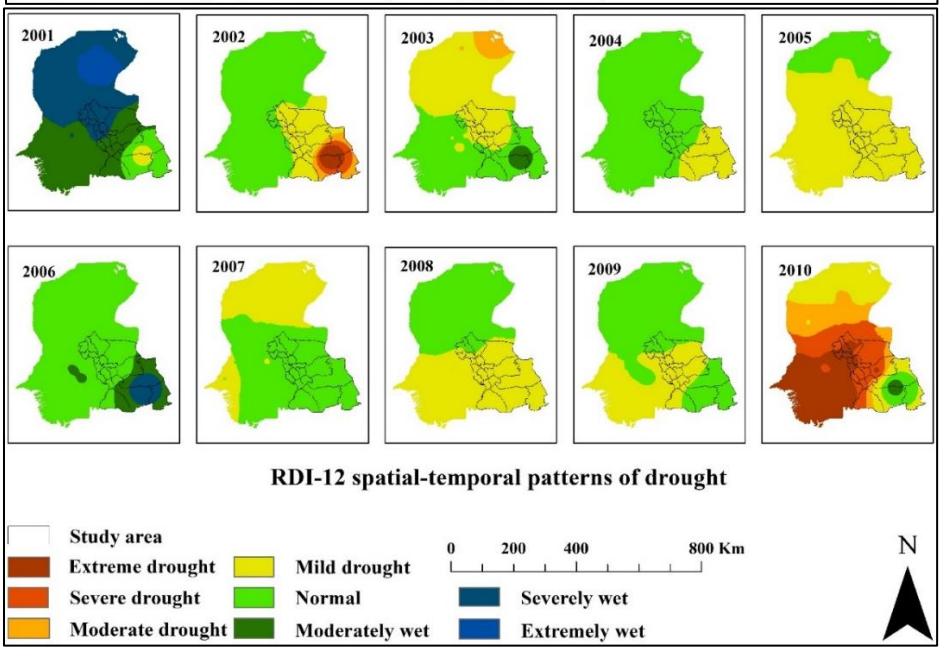
2001
2002
2003
2004
2005
2006
2007
2008
2009
2010
RDI-12 spatial-temporal patterns of drought
Study area
Extreme drought
Severe drought
Moderate drought
Mild drought
Normal
Moderately wet
Severely wet
Extremely wet
0 200 400 800 Km
N

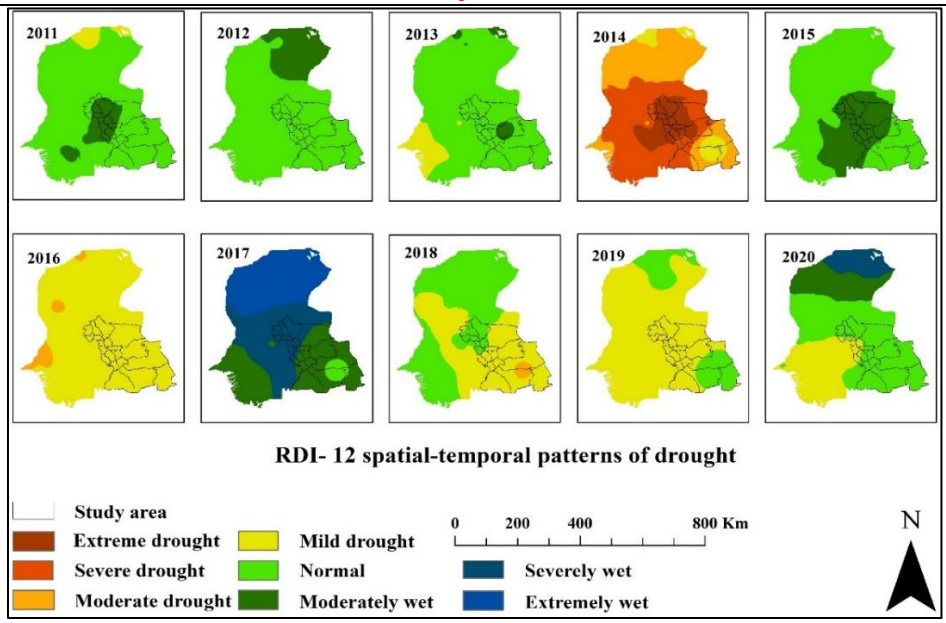

Figure 4: RDI-12 spatial-temporal patterns of drought for the years (1981–2020) based on RDI values

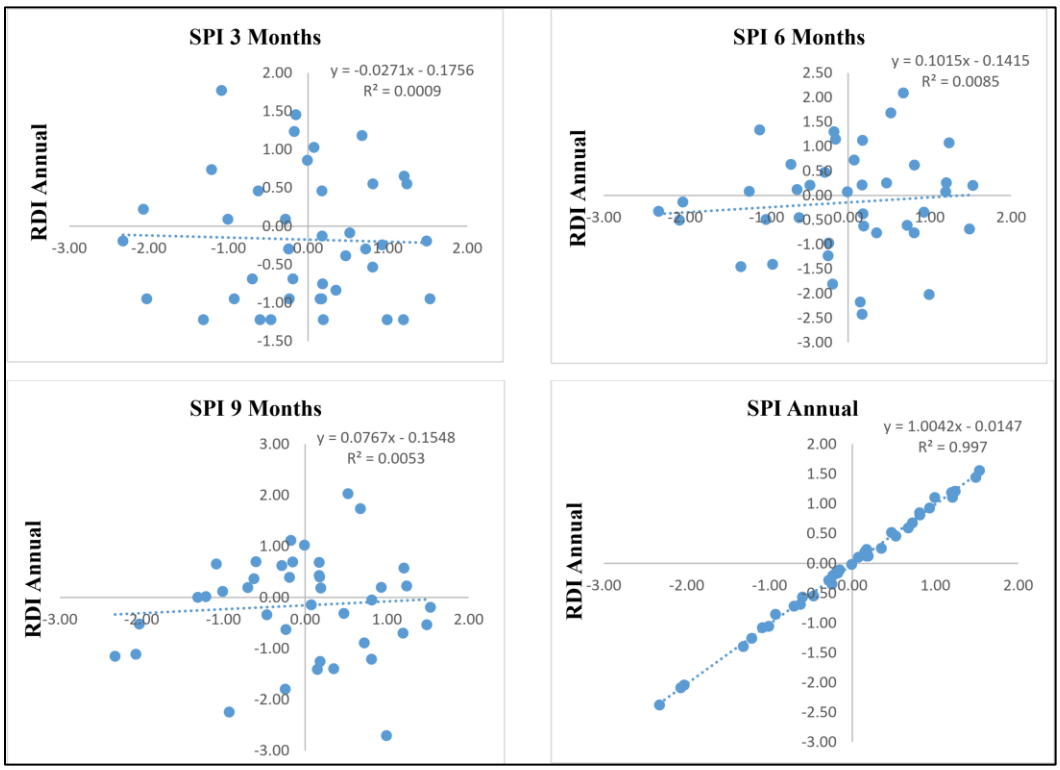

Figure 5: Comparison of SPI 3-, 6-, 9- and 12-months Vs. RDI Annual (Mirpurkhas)

The RDI and SPI indices can be used to estimate drought duration over 3, 6, and 12 months. Figure 5-8 illustrates the linear trend line derived from the strong correlation between RDI and SPI values in the Sindh region. The results highlight a significant relationship between these indices. Even with rainfall data alone, the algorithm applied to the graphs allows for accurate calculation of the RDI and forecasting of drought-prone seasons. In linear regression analysis, the yearly SPI and yearly RDI show a close fit, with an R^2 value of 0.998. Comparisons were made between the first three months, second three months, third and fourth months, first six months, and first nine months of the SPI and the annual RDI values. The best strategies are illustrated in the graphs. The calculations using SPI values from the first nine months, half-year,

and first quarter produced robust results with high R^2 values. These findings suggest that by providing the first three months of rainfall data and calculating the SPI for subsequent years, it is feasible to predict RDI drought indices.

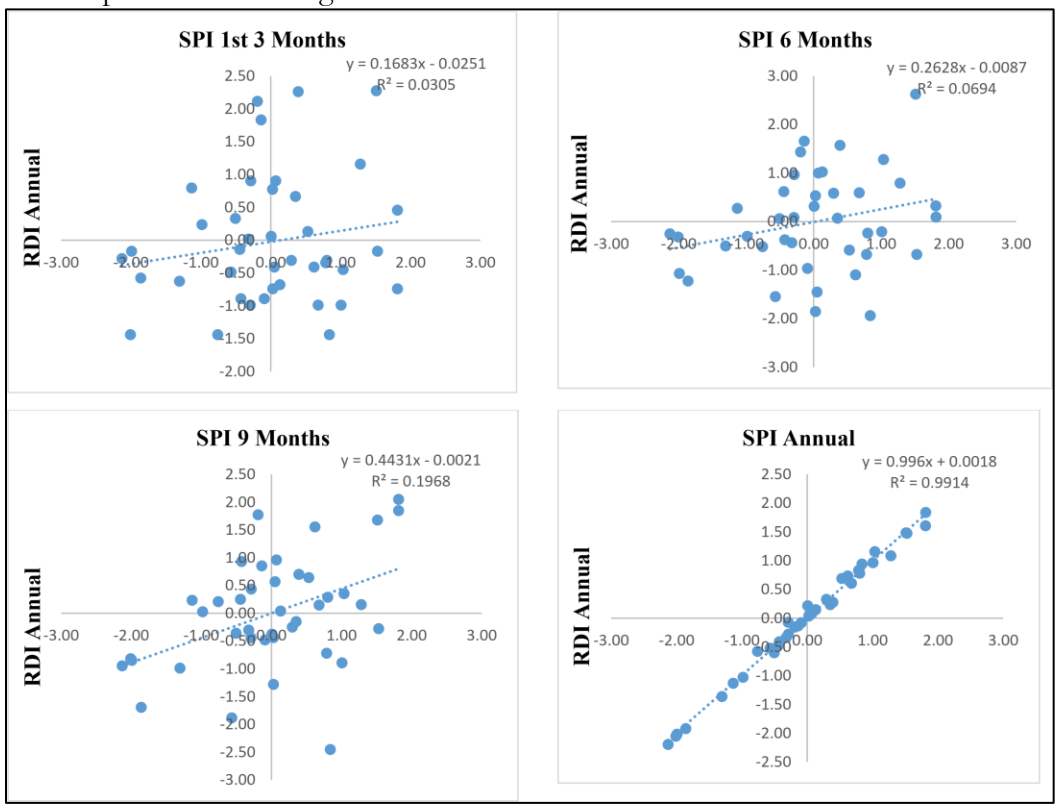

Figure 6: Comparison of SPI 3-, 6-, 9- and 12-months Vs. RDI Annual (Shanghar)

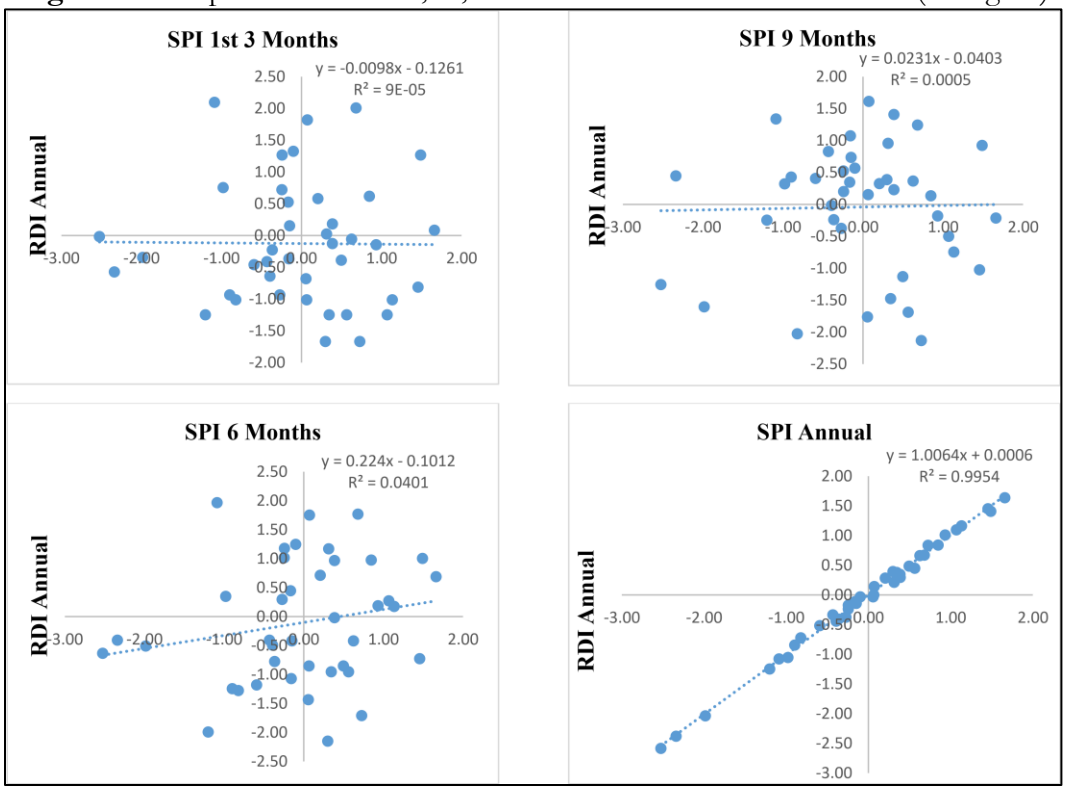

Figure 7: Comparison of SPI 3-, 6-, 9- and 12-months Vs. RDI Annual (Tharparkar)

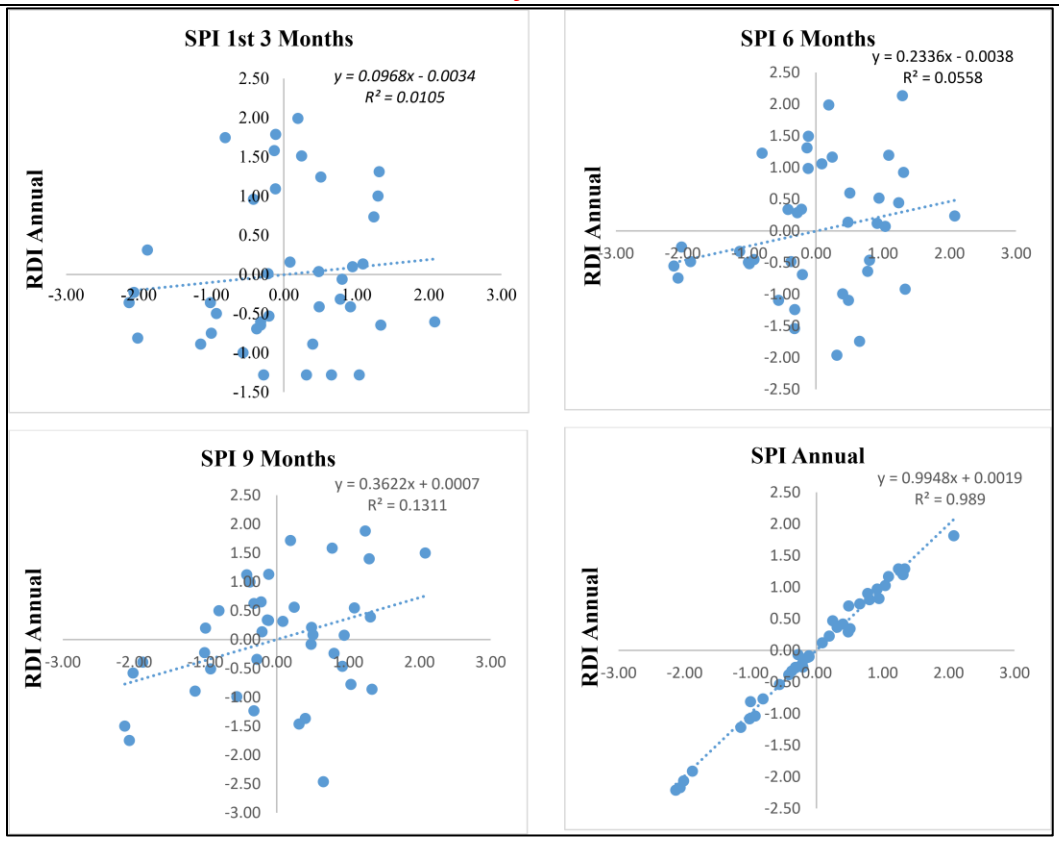

Figure 8: Comparison of SPI 3-, 6-, 9- and 12-months Vs. RDI Annual (Umerkot)

Normalized Difference Vegetation Index (NDVI) Changes:

The NDVI model was developed using Landsat images from 1988, 1998, 2008, 2018, and 2021, with vegetation cover assessed using ArcGIS software. NDVI values in the study area ranged from 0.99 to +0.53 in 1988, 0.78 to +0.81 in 1998, 0.99 to +0.99 in 2008, and 0.75 to +0.49 in 2018. By 2021, NDVI values had shifted to a minimum of 0.2 and a maximum of +0.48. Higher NDVI values typically indicate more productive areas, such as dense vegetation and forests, while lower values correspond to less productive regions like bare soil, water bodies, and built-up areas. The NDVI map reveals a notable decline in the most productive areas over time. Generally, forested regions exhibit higher NDVI values compared to bare soil, suggesting that the expansion of vegetation may have influenced the overall greenness of the area as detected by satellite. A significant change in NDVI values was observed between 1988 and 1998, demonstrating an overall increase in NDVI values in the selected district over time.

Land Surface Temperature (LST) Changes:

Figure 9 illustrates the spatial distribution and areal extent of Land Surface Temperature (LST) across the districts of Shanghar, Umerkot, Tharparkar, and Mirpurkhas for five distinct years—1988, 1998, 2008, 2018, and 2021—with a ten-year interval between each. The spatial patterns reveal significant variations in LST across the study area. In 1988, LST values ranged from 35.16°C to 17.39°C; in 1998, from 53.8°C to -69.40°C; in 2008, from 40.00°C to 24.38°C; in 2018, from 47.54°C to 25.4°C; and in 2021, from 53.44°C to 25.77°C. Over the period from 1988 to 2021, the study area experienced a decrease in vegetation and an increase in built-up areas, leading to a rise in LST. The northern part of the region, such as Shanghar, retains a lower temperature due to its higher vegetation and agricultural land. Conversely, the central area, including Umerkot, shows increased LST due to accelerated urbanization and a decline in water bodies and vegetation. The discrepancy between estimated and recorded LST values is within acceptable limits, considering the constraints of RS-derived LST estimation. These results are valuable for future analyses, including LST simulation and temperature condition indexing.

Additionally, September, according to Pakistan's agricultural calendar, is a period of substantial vegetation cover, during which maximum LST values were assessed for the study area.

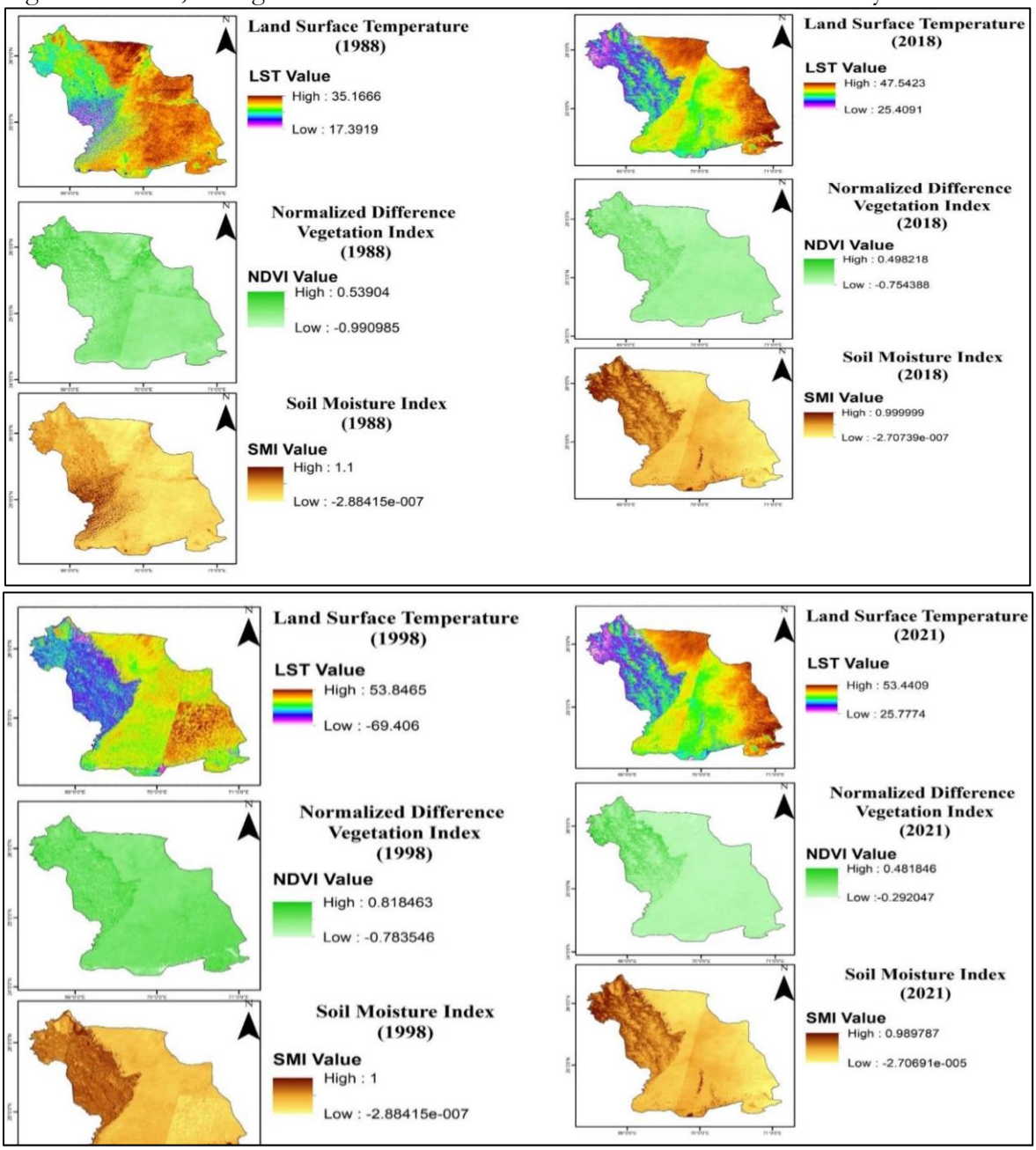

Figure 9: Spatio-temporal analysis of LST, NDVI and SMI in 1988, 1998, 2008, 2018 and 2021

Soil Moisture Index (SMI) Change:

The Soil Moisture Index (SMI) ranges from 0 to 1, where 0 indicates the lowest soil moisture and 1 signifies the highest. This index reflects the relative amount of soil moisture on a given date. Without calibration of the soil moisture measurements, quantitative comparisons across different days within the chosen month of September are not possible. The graph indicates that soil moisture levels were high in 1988 and subsequent years; however, by 2018, the SMI had declined to 0.99, and it further decreased to 0.98 three years later.

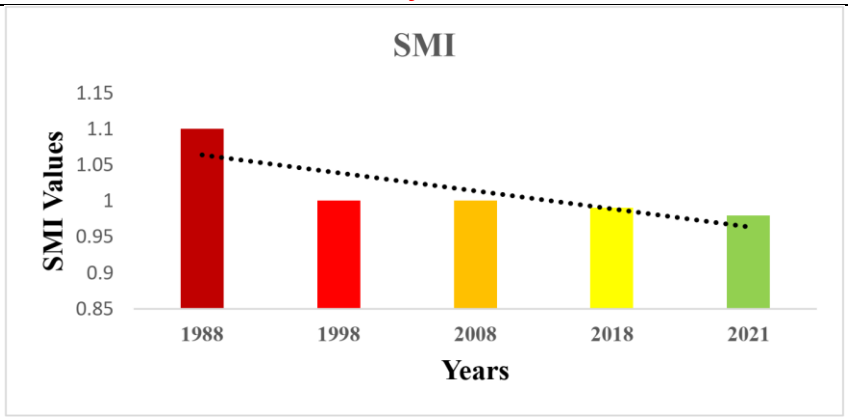

Figure 10: Graph showing the trendline of SMI values for the month of September in the years 1988, 1989, 2008, 2018, and 2021.

Relationship between LST and NDVI:

Figure 11 illustrates the comparative analysis between NDVI and LST, highlighting a strong inverse relationship between the two. The trend line clarifies that as NDVI decreases, indicating reduced vegetation, LST increases. This negative relationship suggests that areas with greater vegetation biomass tend to have lower LST. The direct correlation between LST and NDVI reflects changes in land cover. Specifically, images with lower NDVI values, characteristic of barren soil in the Thar desert, show less vegetation and higher LST. Conversely, areas with higher NDVI values, indicating dense vegetation, experience lower LST due to the cooling effect of abundant plant cover.

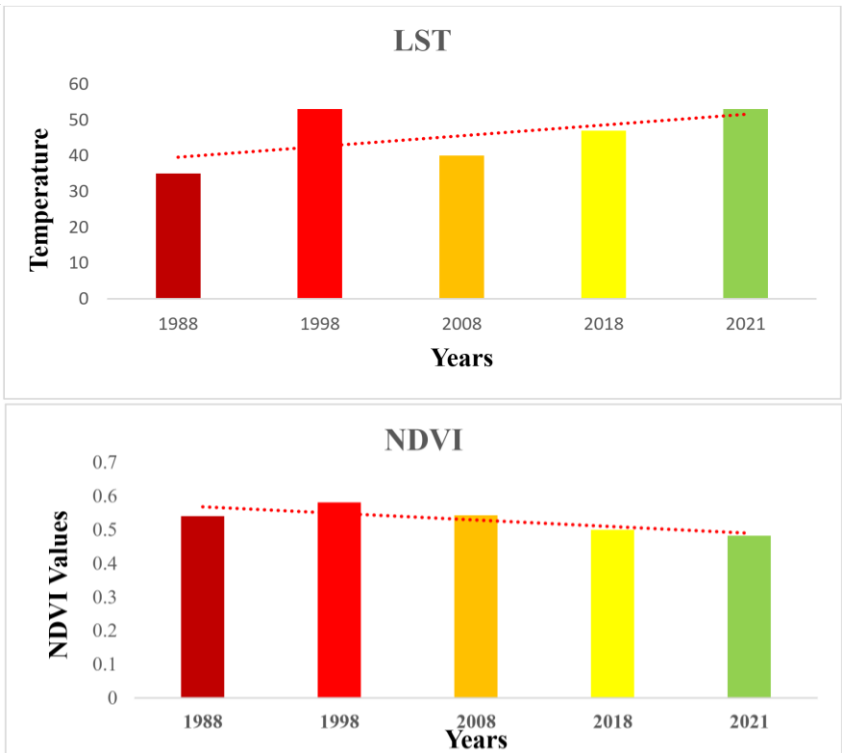

Figure 11: Graph showing the comparison between the trends of NDVI and LST values in the years 1988, 1989, 2008, 2018, and 2021.

There is a significant direct correlation between LST and NDVI, enabling the prediction of LST through direct regression if NDVI values for the research area are known. Consequently, NDVI can be used to estimate precise LST values. Analysis from 1988 to 2021 reveals a decline in NDVI values due to urban expansion and reduced vegetation. This correlation also helps differentiate between high LST areas, typically characterized by bare soil, and low temperature

areas with more vegetation. The highest LST values correspond to the lowest NDVI, and vice versa.

Conclusion:

Droughts, driven by insufficient water resources, are among the most common natural disasters adversely affecting crop productivity. Between 1981 and 2020, RDI and SPI were assessed every three, six, and twelve months at four meteorological stations in Sindh, Pakistan. The drought characterization over this 40-year period revealed 4-6 years of moderate to severe drought. Specifically, the three-month RDI data indicated extreme, severe, and moderate drought episodes occurring every four to six years. The study also evaluated the accuracy and applicability of SPI and RDI in Sindh, highlighting how temperature deviations have led to reduced precipitation, extended dry spells, and diminished freshwater supplies for irrigation, directly impacting agricultural development.

The SPI measures deviations from the long-term average of a normally distributed variable, being positive when precipitation exceeds the average and negative otherwise. Low SPI values indicate dry conditions. Regression results show a strong correlation between SPI and RDI, allowing for the estimation of annual RDI drought indicators from initial three-month precipitation data. The continuous decline in RDI time-series data indicates increasing drought severity. Long-term droughts pose a risk to water resource management, particularly affecting groundwater quality. In summary, the study highlights significantly low NDVI and SMI values along with high LST across the study period. These findings provide crucial insights for ongoing land monitoring and are essential for policymakers aiming to enhance land resource management strategies. The results will aid regional policymakers in developing comprehensive land management plans at both regional and national levels.

References:

[1] J. M. Kirby et al., "The impact of climate change on regional water balances in Bangladesh," Clim. Change, vol. 135, no. 3–4, pp. 481–491, Apr. 2016, doi: 10.1007/S10584-016-1597-1/METRICS.

[2] P. Kumar, S. F. Shah, M. A. Uqaili, L. Kumar, and R. F. Zafar, "Forecasting of Drought: A Case Study of Water-Stressed Region of Pakistan," Atmos. 2021, Vol. 12, Page 1248, vol. 12, no. 10, p. 1248, Sep. 2021, doi: 10.3390/ATMOS12101248.

[3] G. Gebremeskel Haile et al., "Long-term spatiotemporal variation of drought patterns over the Greater Horn of Africa," Sci. Total Environ., vol. 704, p. 135299, Feb. 2020, doi: 10.1016/J.SCITOTENV.2019.135299.

[4] Y. Mao, Z. Wu, H. He, G. Lu, H. Xu, and Q. Lin, "Spatio-temporal analysis of drought in a typical plain region based on the soil moisture anomaly percentage index," Sci. Total Environ., vol. 576, pp. 752–765, Jan. 2017, doi: 10.1016/J.SCITOTENV.2016.10.116.

[5] M. Waseem, A. H. Jaffry, M. Azam, I. Ahmad, A. Abbas, and J. E. Lee, "Spatiotemporal Analysis of Drought and Agriculture Standardized Residual Yield Series Nexuses across Punjab, Pakistan," Water 2022, Vol. 14, Page 496, vol. 14, no. 3, p. 496, Feb. 2022, doi: 10.3390/W14030496.

[6] T. Jiang, X. Su, V. P. Singh, and G. Zhang, "Spatio-temporal pattern of ecological droughts and their impacts on health of vegetation in Northwestern China," J. Environ. Manage., vol. 305, p. 114356, Mar. 2022, doi: 10.1016/J.JENVMAN.2021.114356.

[7] S. Adnan, K. Ullah, A. H. Khan, and S. Gao, "Meteorological impacts on evapotranspiration in different climatic zones of Pakistan," J. Arid Land, vol. 9, no. 6, pp. 938–952, Dec. 2017, doi: 10.1007/S40333-017-0107-2/METRICS.

[8] U. Surendran, V. Kumar, S. Ramasubramoniam, and P. Raja, "Development of Drought Indices for Semi-Arid Region Using Drought Indices Calculator (DrinC) – A Case Study from Madurai District, a Semi-Arid Region in India," Water Resour. Manag., vol. 31, no. 11, pp. 3593–3605, Sep. 2017, doi: 10.1007/S11269-017-1687-5/METRICS.

[9] S. Mukherjee, S. Aadhar, D. Stone, and V. Mishra, "Increase in extreme precipitation events under anthropogenic warming in India," Weather Clim. Extrem., vol. 20, pp. 45–53, Jun. 2018, doi: 10.1016/J.WACE.2018.03.005.

[10] S. Hina, F. Saleem, A. Arshad, A. Hina, and I. Ullah, "Droughts over Pakistan: possible cycles, precursors and associated mechanisms," Geomatics, Nat. Hazards Risk, vol. 12, no. 1, pp. 1638–1668, 2021, doi: 10.1080/19475705.2021.1938703.

[11] C. Cammalleri, F. Micale, and J. Vogt, "A novel soil moisture-based drought severity index (DSI) combining water deficit magnitude and frequency," Hydrol. Process., vol. 30, no. 2, pp. 289–301, Jan. 2016, doi: 10.1002/HYP.10578.

[12] N. Sánchez, Á. González-Zamora, M. Piles, and J. Martínez-Fernández, "A New Soil Moisture Agricultural Drought Index (SMADI) Integrating MODIS and SMOS Products: A Case of Study over the Iberian Peninsula," Remote Sens. 2016, Vol. 8, Page 287, vol. 8, no. 4, p. 287, Mar. 2016, doi: 10.3390/RS8040287.

[13] S. Fahad et al., "Crop production under drought and heat stress: Plant responses and management options," Front. Plant Sci., vol. 8, p. 265598, Jun. 2017, doi: 10.3389/FPLS.2017.01147/BIBTEX.

[14] N. Salehnia, A. Alizadeh, H. Sanaeinejad, M. Bannayan, A. Zarrin, and G. Hoogenboom, "Estimation of meteorological drought indices based on AgMERRA precipitation data and station-observed precipitation data," J. Arid Land, vol. 9, no. 6, pp. 797–809, Dec. 2017, doi: 10.1007/S40333-017-0070-Y/METRICS.

[15] Q. Liu et al., "Evaluating the performance of eight drought indices for capturing soil moisture dynamics in various vegetation regions over China," Sci. Total Environ., vol. 789, p. 147803, Oct. 2021, doi: 10.1016/J.SCITOTENV.2021.147803.

[16] K. Xu, D. Yang, H. Yang, Z. Li, Y. Qin, and Y. Shen, "Spatio-temporal variation of drought in China during 1961–2012: A climatic perspective," J. Hydrol., vol. 526, pp. 253–264, Jul. 2015, doi: 10.1016/J.JHYDROL.2014.09.047.

[17] D. Tigkas, H. Vangelis, and G. Tsakiris, "DrinC: a software for drought analysis based on drought indices," Earth Sci. Informatics, vol. 8, no. 3, pp. 697–709, Sep. 2015, doi: 10.1007/S12145-014-0178-Y/METRICS.

[18] D. Tigkas, H. Vangelis, and G. Tsakiris, "An enhanced effective reconnaissance drought index for the characterisation of agricultural drought," Environ. Process., vol. 4, no. 1, pp. S137–S148, Nov. 2017, doi: 10.1007/S40710-017-0219-X/METRICS.

[19] A. Saha, M. Patil, V. C. Goyal, and D. S. Rathore, "Assessment and Impact of Soil Moisture Index in Agricultural Drought Estimation Using Remote Sensing and GIS Techniques," Proc. 2019, Vol. 7, Page 2, vol. 7, no. 1, p. 2, Nov. 2018, doi: 10.3390/ECWS-3-05802.

[20] W. Li et al., "Spatiotemporal characteristics of drought in a semi-arid grassland over the past 56 years based on the Standardized Precipitation Index," Meteorol. Atmos. Phys., vol. 133, no. 1, pp. 41–54, Feb. 2021, doi: 10.1007/S00703-020-00727-4/METRICS.

[21] T. Iwata et al., "Preoperative serum value of sialyl Lewis X predicts pathological nodal extension and survival in patients with surgically treated small cell lung cancer," J. Surg. Oncol., vol. 105, no. 8, pp. 818–824, Jun. 2012, doi: 10.1002/JSO.23002.

[22] D. Lang et al., "A Comparative Study of Potential Evapotranspiration Estimation by Eight Methods with FAO Penman–Monteith Method in Southwestern China," Water 2017, Vol. 9, Page 734, vol. 9, no. 10, p. 734, Sep. 2017, doi: 10.3390/W9100734.

[23] M. A. Asadi Zarch, B. Sivakumar, H. Malekinezhad, and A. Sharma, "Future aridity under conditions of global climate change," J. Hydrol., vol. 554, pp. 451–469, Nov. 2017, doi: 10.1016/J.JHYDROL.2017.08.043.

[24] S. Sruthi and M. A. M. Aslam, "Agricultural Drought Analysis Using the NDVI and Land Surface Temperature Data; a Case Study of Raichur District," Aquat. Procedia,

vol. 4, pp. 1258–1264, Jan. 2015, doi: 10.1016/J.AQPRO.2015.02.164.

[25] A. R. Zarei, "Analysis of changes trend in spatial and temporal pattern of drought over south of Iran using standardized precipitation index (SPI)," SN Appl. Sci., vol. 1, no. 5, pp. 1–14, May 2019, doi: 10.1007/S42452-019-0498-0/TABLES/6.

[26] H. C. Kraemer and C. Blasey, "How Many Subjects?: Statistical Power Analysis in Research," How Many Subj. Stat. Power Anal. Res., Jan. 2016, doi: 10.4135/9781483398761.

[27] M. Ben Abdelmalek and I. Nouiri, "Study of trends and mapping of drought events in Tunisia and their impacts on agricultural production," Sci. Total Environ., vol. 734, p. 139311, Sep. 2020, doi: 10.1016/J.SCITOTENV.2020.139311.

[28] M. A. Amini, G. Torkan, S. Eslamian, M. J. Zareian, and J. F. Adamowski, "Correction to: Analysis of deterministic and geostatistical interpolation techniques for mapping meteorological variables at large watershed scales (Acta Geophysica, (2019), 67, 1, (191-203), 10.1007/s11600-018-0226-y)," Acta Geophys., vol. 67, no. 1, p. 275, Feb. 2019, doi: 10.1007/S11600-018-0235-X/METRICS.